Optical Engineering

OpticalEngineering.SPIEDigitalLibrary.org

Enhancement of optical absorption in silicon thin-film solar cells with metal nanoparticles

Bo Shi
Wei Wang
Xueqing Yu
Lili Yang
Yuanpei Xu

SPIE.

Bo Shi, Wei Wang, Xueqing Yu, Lili Yang, Yuanpei Xu, "Enhancement of optical absorption in silicon thin-film solar cells with metal nanoparticles," *Opt. Eng.* **56**(5), 057105 (2017), doi: 10.1117/1.OE.56.5.057105.

Enhancement of optical absorption in silicon thin-film solar cells with metal nanoparticles

Bo Shi,* Wei Wang, Xueqing Yu, Lili Yang, and Yuanpei Xu
Nanjing University of Aeronautics and Astronautics, College of Energy and Power Engineering, Nanjing, China

Abstract. Light trapping structures are a promising method of improving the efficiency of solar cells. We focused on the plasmonic thin-film solar cell. A structure is proposed consisting of an indium tin oxide layer with embedded metal nanoparticles, a hydrogenated amorphous silicon (a-Si:H) layer, and an aluminum (Al) layer. The finite-difference-time-domain (FDTD) method was used to calculate the absorption characteristics of the a-Si:H thin-film solar cells containing nanoparticles. By arranging the material, size, and locations of metal nanoparticles to maximize the scattering and minimize absorption of nanoparticles themselves, the optical absorption in the solar cell is significantly enhanced. [DOI: 10.1117/1.OE.56.5.057105]

Keywords: thin-film solar cells; metal nanoparticles; surface plasmon.

Paper 170279 received Feb. 27, 2017; accepted for publication May 1, 2017; published online May 17, 2017.

1 Introduction

Thin-film solar cells are a promising alternative to bulk crystalline silicon solar cells;[1] however, the absorption coefficient of incident light around the band gap of silicon is low. Therefore, trapping light is crucial to increasing the performance of thin-film solar cells and can make them competitive with crystalline silicon solar cells.[2] Previous work has proposed a variety of light-trapping techniques, such as gratings,[3–5] nanostructures,[6–8] refractive index matching,[9] and reduction of surface plasmonic absorption.[10,11] Recent experiments found that metal nanoparticles can induce the plasmonic effect and are a promising approach to achieving light trapping in thin-film solar cells. The nanoparticles can increase the optical path length in a thin-film solar cell by scattering the incident light into the active layer effectively.[11]

The optical properties of metal nanoparticles are sensitive to their size and shape, the surface coverage on the substrate, and the surrounding medium.[12–14] The light can be either scattered or absorbed by metal nanoparticles; therefore, the nanoparticles must be well designed to maximize the scattering and minimize absorption across the wavelength range of interest. Silver nanoparticles (Ag NPs),[15] aluminum nanoparticles (Al NPs),[16,17] gold nanoparticles (Au NPs),[18,19] and copper nanoparticles (Cu NPs)[20] are commonly studied because of their unique optical properties.

The structure of hydrogenated amorphous silicon (a-Si:H) thin-film solar cell, with metal nanoparticles embedded in an indium tin oxide (ITO) layer and an Al layer on the backside (considered as both the back reflector and the electrode), is investigated in this paper. This design can optimize light absorption across the wavelength range of interest in solar cells. It is of great importance for evaluating the factors that have an influence on the optical absorption of solar cells. Based on the analysis of the material and size of the embedded nanoparticles, we also studied the arrangement of nanoparticles to realize absorption enhancement in the active layer in comparison with the previous studies.[16,21–23]

2 Structure and Method

The proposed structure, shown in Fig. 1, consists of a 250-nm-thick a-Si:H layer, a 70-nm-thick ITO layer, and a 70-nm-thick Al layer. We assumed that the metal nanoparticles with period $p = 150$ nm, which are in contact with the a-Si:H layer, are embedded in the ITO coating.

For the numerical experiments, we used the finite-difference-time-domain (FDTD) method to solve a full set of three-dimensional Maxwell equations with perfectly matched layer boundary conditions for normally incident planar waves. The FDTD method yields discrete equations that are obtained in the Yee cell from Maxwell's curl equations. The electric and magnetic field samples are obtained in the time domain, and the sampling interval between the electric and magnetic fields is a half-step in the time domain. The electric and magnetic fields are obtained by an iterative solver combined with the initial conditions and boundary conditions. Maxwell's curl equations are[24]

$$\nabla \times H = \frac{\partial D}{\partial t} + J, \tag{1}$$

$$\nabla \times E = -\frac{\partial D}{\partial t} - J_m, \tag{2}$$

$$D = \varepsilon E, \tag{3}$$

$$B = \mu H, \tag{4}$$

where H is the magnetic field, E is the electric field, B is the magnetic flux intensity, D is the electric flux intensity, J is the current density, J_m is the magnetic density, t is the time, μ is the complex permeability, and ε is the complex permittivity. In a rectangular coordinate system, the central difference method can be used to approximately replace the first-order partial derivative of the electric and magnetic fields on the space domain and time domain to discretize the electric

*Address all correspondence to: Bo Shi, Email: boshi@nuaa.edu.cn

0091-3286/2017/$25.00

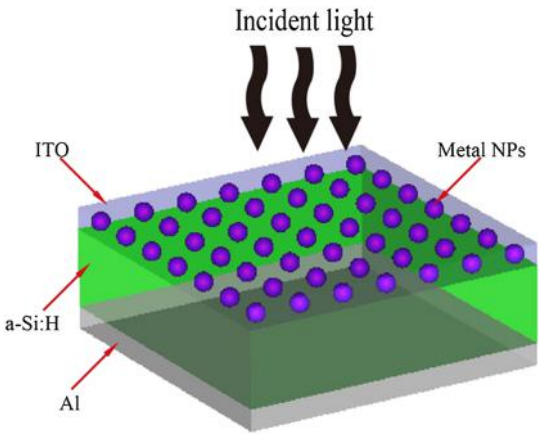

Fig. 1 Sketch of the thin-film solar cell structure, consisting of a 250-nm-thick a-Si:H layer, a 70-nm-thick Al layer, and a 70-nm-thick ITO layer with the metal nanoparticles thereon.

and magnetic fields, respectively, in the space and time domains.[25] Therefore, numerical calculation of the structure can be performed according to the electromagnetic parameters of the nodes next to the boundary after meshing the simulation region. The structure used in this work assumed that all the energy through the surface could be absorbed. Simulations were performed for a square array of nanoparticles by applying periodic boundary conditions. The performed simulations took into account all the major effects of the metal nanoparticles deposited on the top cell. Refractive index data for the a-Si:H and Al used in the simulation were obtained from Ref. 26, and the ITO data were obtained from the SOPRA database. The reflectivity, transmission, and absorption rate of a solar cell can be obtained by the electric field of the incident electromagnetic wave.

There is a great difference in absorption characteristics for different microstructures. Here, we discuss the absorption characteristics of solar cells with embedded nanoparticles. It is of great importance to find the optimal nanoparticle parameters, including the material, shape, and size, to enhance the optical absorption and efficiency of solar cells. These parameters also determine the scattering efficiency and spectral response of micro- and nanostructures.

3 Results and Discussion

3.1 *Material Optimization*

For convenience, we normalized the incident light power to unity. Figure 2(a) shows the absorption characteristics of solar cells embedded with the different metal nanoparticles in the visible wavelength range, demonstrating that the absorption of solar cells with metal nanoparticles increases significantly and that both the peak position and value of absorption also change compared to that without metal nanoparticles. The absorption enhancement of different metal nanoparticles is presented in Fig. 2(b). The absorption enhancement is the ratio of the difference between the absorption with and without nanoparticles to the absorption without nanoparticles. As can be seen from Fig. 2(b), Al nanoparticles, which mainly enhance the absorption over 300 to 500 nm, provide the strongest absorption enhancement among the four kinds of metal nanoparticles.

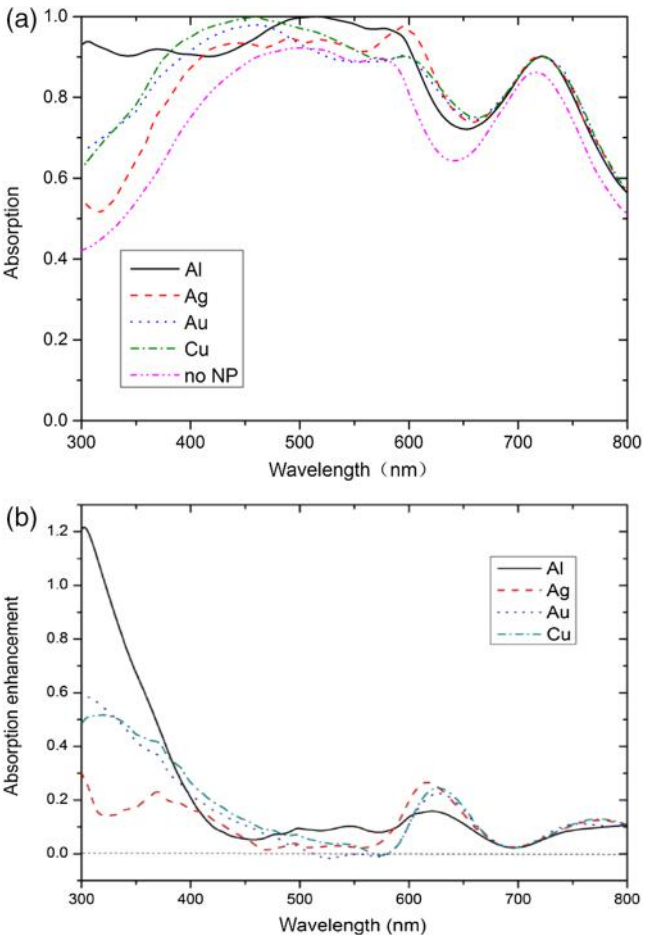

Fig. 2 (a) Absorption and (b) absorption enhancement of solar cells embedded with Al, Ag, Au, Cu nanoparticles, for radius 30 nm, period 150 nm. "no NP" indicates the absorption without nanoparticles.

The spectral absorption rate is defined as

$$A(\lambda) = \frac{\int \mathrm{abs}(\lambda) I(\lambda) \mathrm{d}\lambda}{\int I(\lambda) \mathrm{d}\lambda}, \tag{5}$$

where λ is the wavelength, $\mathrm{abs}(\lambda)$ is the absorption rate from simulation, and $I(\lambda)$ is the spectral irradiance. As shown in Table 1, the deposition of metal nanoparticles on the surface of the solar cells can effectively improve the spectral absorption rate. Furthermore, the enhanced ratio of average

Table 1 Average absorption and the enhanced ratio of average absorption of different metal nanoparticles.

Metal nanoparticles	Average absorption	Enhanced ratio of average absorption (%)
no NP	0.7904	—
Al	0.8802	11.3613
Ag	0.8591	8.6918
Au	0.8621	9.0714
Cu	0.868	9.8178

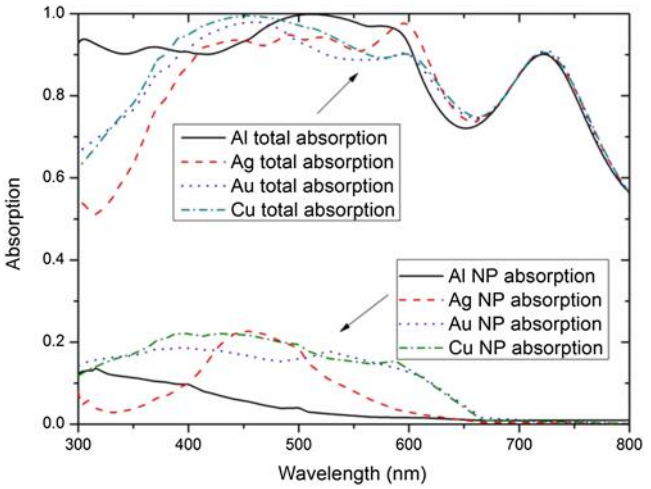

Fig. 3 Absorption of the whole structure with Al, Ag, Au, Cu nanoparticles and absorption of the nanoparticles themselves, for radius 30 nm, period 150 nm.

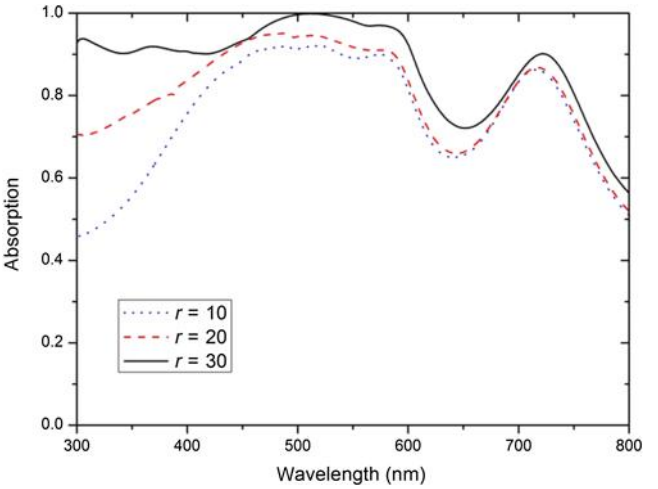

Fig. 4 Absorption of solar cells embedded with Al nanoparticles as the radius is 10, 20, or 30 nm, where $p = 150$ nm.

absorption of Al particles, up to 11%, is the highest. The incident light path length in the active layer can be enhanced by scattering the electromagnetic wave with short wavelength by metal nanoparticles, thereby improving the optical absorption rate inside the photoactive layer. In addition, the localized surface plasmons of Al NPs appear when short wavelengths of light are present and, thus, reduce the excitation loss in the Al NPs.

Based on the former calculation, we have a preliminary understanding of optical absorption of thin-film solar cells. In fact, the resonance coupling between incident light and surface plasmons can also lead to parasitic absorption of nanoparticles.[27] Optical absorption of the photoactive layer is similar to the difference between the total absorption and the parasitic absorption of metal nanoparticles themselves; thus, the true value of the optical absorption will be slightly reduced. Figure 3 shows that the parasitic absorption of Al and Ag nanoparticles is weaker than the others in the visible range.

To maximize the coupling efficiency of the active layer, it is necessary to increase the energy that transfer into the active layer and reduce the parasitic absorption of the nanoparticles themselves in the largest intensity region of the irradiation spectrum. Ag nanoparticles are a great choice for optimizing metallic nanostructures of thin-film solar cells.[12] As the surface plasmon resonance frequency of Al nanoparticles is greater than the visible spectrum, Al nanoparticles are superior to Ag nanoparticles owing to the smaller parasitic absorption. Moreover, the high electron density and the large negative permittivity of Al give it favorable scattering on the surface. Based on this, we believe Al nanoparticles can be used to increase photon absorption and improve the photocurrent more than noble metal nanoparticles.

3.2 *Size Optimization*

In Sec. 3.1, the type of metal particles was discussed. In this section, we analyze the absorption characteristics of different sizes of nanoparticles. Al nanoparticles were chosen and embedded in the ITO layer, as per the locations shown in Fig. 1. Figure 4 shows the absorption of solar cells with different sizes of nanoparticles. Clearly, the larger the nanoparticle is, the stronger the absorption becomes in the wavelengths between 300 and 800 nm. Furthermore, the enhanced absorption is even greater within the wavelengths between 300 and 650 nm.

Table 2 Average absorption and the enhanced ratio of average absorption of solar cells with different sizes.

Nanoparticle radius (nm)	Average absorption	Enhanced ratio of average absorption (%)
no NP	0.7904	—
10	0.7934	0.3796
20	0.8260	4.504
30	0.8802	11.3613

It can be concluded from Table 2 that the size of the deposited metal nanoparticles has a large influence on the surface spectrum absorption rate of the solar cell. Specifically, the absorption enhancement effect becomes more and more apparent as the radius increases. The absorption enhancement shows little change with a radius of 10 nm, while the enhanced spectral absorption rate reaches 11% with a radius of 30 nm. Because the ITO layer is 70-nm-thick, the radius of the particles was limited to 30 nm.

Optimizing scattering and absorption of the sunlight by the surface plasmon modes explains why the maximum enhancement is higher for larger nanoparticles. The higher-order plasma modes of large nanoparticles have stronger forward scattering, which can more efficiently trap the light inside the amorphous silicon layer.[27]

3.3 *Arrangement Optimization*

Four locations of Al nanoparticles were designed, as shown in Fig. 5(a). Figure 5(b) shows the absorption of the solar cell with the nanoparticles in the four different positions.

Comparing the curves of "C" and "no NP" in Fig. 5(b), it is found that nanoparticles embedded in the active layer have little impact on the absorption of the wavelengths

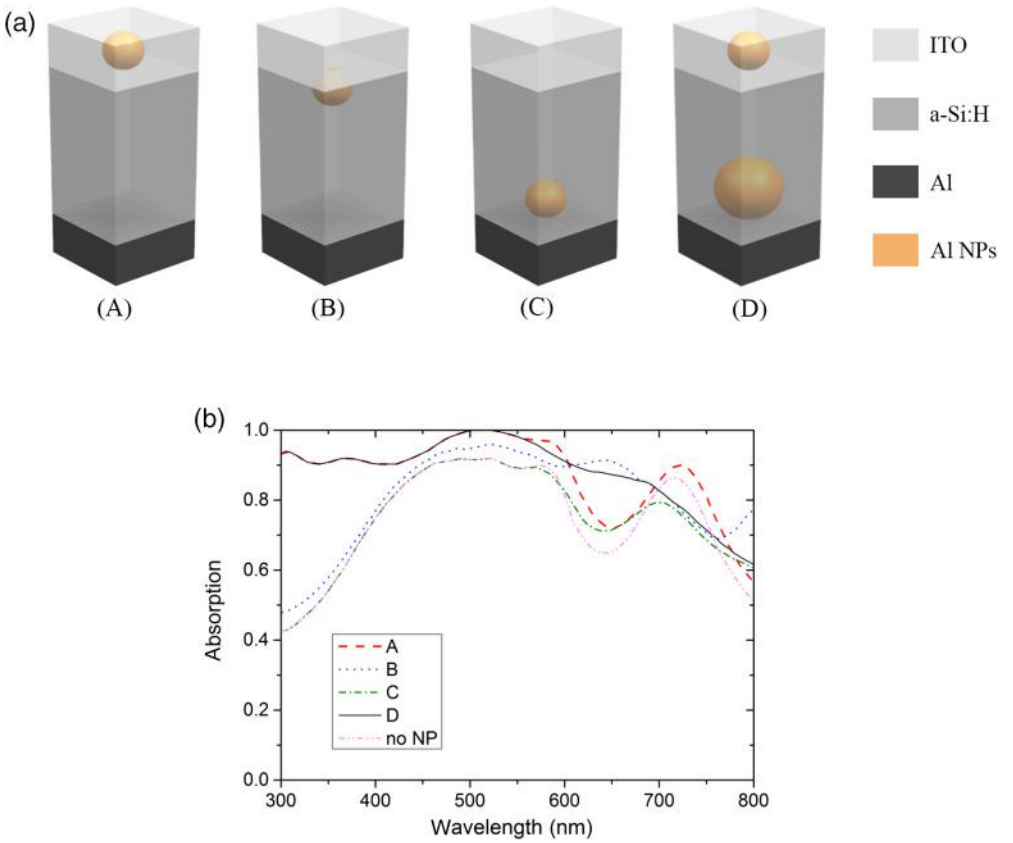

Fig. 5 (a) Four structures of periodic unit cell for simulation: an Al particle with a radius of 30 nm (A) at the bottom of the ITO layer, (B) at the top of the a-Si:H layer, (C) at the bottom of the a-Si:H layer, and (D) at the bottom of the ITO layer and another Al particle with a radius of 50 nm at the bottom of the a-Si:H layer; (b) absorption of the solar cell in the four different structures above.

from 300 to 550 nm. In fact, it can only affect absorption at wavelengths greater than 550 nm. Because there are no particles on the surface, the high-frequency photons have the same absorption mechanism in the upper layer of a-Si:H; therefore, the absorption rate remains almost unchanged. Low-frequency photons that reach the bottom of the solar cells are not completely absorbed. However, if metal nanoparticles are present in the bottom, they will scatter more light and have a greater chance of improving absorption.

Comparing the curves of "A," "C," and "no NP," it is found that nanoparticles in the ITO layer "A" can increase the absorption from 300 to 600 nm, while nanoparticles embedded on the bottom of a-Si:H layer "C" can optimize the absorption from 550 to 800 nm. Therefore, we propose combining these two types of structures, forming a composite increased structure, namely, nanoparticles embedded in two positions: on the bottom of the ITO layer and the bottom of the a-Si:H layer.

Table 3 shows that the average absorption enhancement of metal nanoparticles deposited on the bottom of a-Si:H layer, which is shown in Fig. 5(a) as structure C, is one order of magnitude smaller than that of metal nanoparticles deposited in other locations.

The radius of nanoparticles on the bottom of the a-Si:H layer was optimized. It is found that when the radius of Al nanoparticles on the bottom of the ITO layer is 30 nm and the radius of Al particles on the bottom of a-Si:H layer is 50 nm, which is shown in Fig. 5(a)(D), silicon thin-film solar cells can obtain the optimal absorption properties over 300 to 800 nm, and the enhanced ratio of average absorption can reach up to 12.4%.

The scattering of the incident light by nanoparticles in structure D is further explained in Fig. 6. Figure 6(a) shows that the strongest scattering of the nanoparticles in the ITO layer appears at the wavelength of 500 nm, which is consistent with the peak of curve "A" in Fig. 5(b). Since the nanoparticles in the ITO layer are the only factor of scattering light within the wavelengths from 300 to 500 nm, the curves "A" and "D" are coincident in Fig. 5(b). While the wavelength is greater than 550 nm, the nanoparticles embedded

Table 3 Absorption of the solar cell with nanoparticles at different positions.

Nanoparticle position	Average absorption	Enhanced ratio of average absorption (%)
no NP	0.7904	—
A	0.8802	11.36134
B	0.8542	8.071862
C	0.7942	0.480769
D	0.8881	12.36083

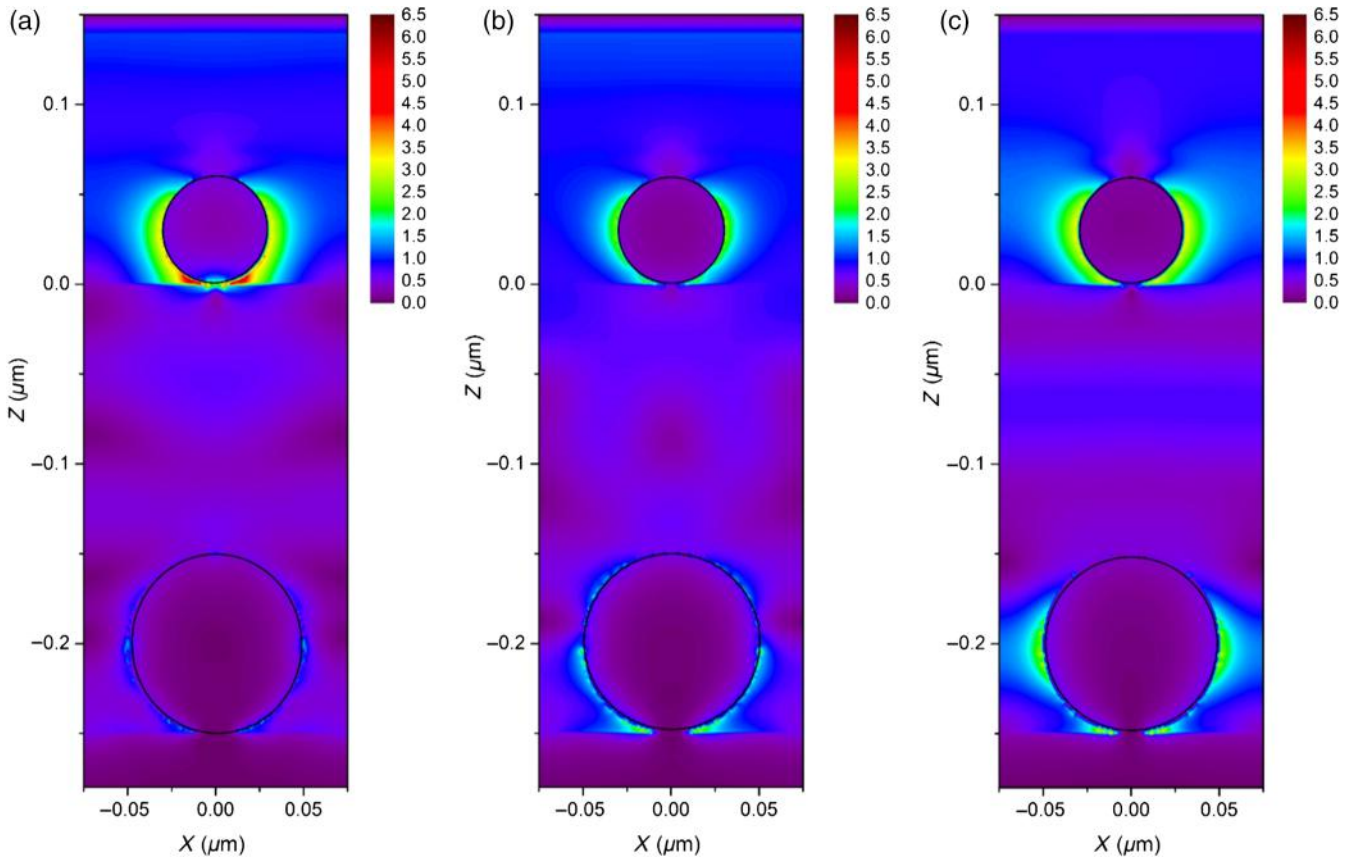

Fig. 6 Electric field distribution in $x-z$ cross section of a periodic unit cell at wavelength (a) 500 nm, (b) 550 nm, and (c) 650 nm. The radiuses of Al NPs in ITO and a-Si:H layers are 30 and 50 nm, respectively.

in the bottom of the active layer are involved in scattering of light, which is shown in Fig. 6(b). It can be seen from Fig. 6(c) that the two particles work together at 650 nm, thus improving the absorption in comparison with the situation of only one particle working alone [curves "A" and "C" in Fig. 5(b)].

3.3.1 *Mie theory*

The conclusion that structure A is better than B in Fig. 5(a) can be explained by Mie theory.[28] The efficiency of absorption and scattering Q_{abs} and Q_{sca} can be calculated via

$$Q_{\text{abs}} = C_{\text{abs}}/\pi r^2, \tag{6}$$

$$Q_{\text{sca}} = C_{\text{sca}}/\pi r^2, \tag{7}$$

$$\alpha = 4\pi r^3 \frac{\varepsilon - \varepsilon_m}{\varepsilon + \varepsilon 2_m}, \tag{8}$$

where C_{abs} and C_{sca} are the absorption and scattering cross sections, respectively, which are associated with the polarizability α,[29] ε is the dielectric constant of metal NPs, ε_m is the dielectric constant of the surrounding medium, which is isotropic and nonabsorbing, and r is the radius of the particle.

C_{abs} and C_{sca} can be calculated via[30]

$$C_{\text{abs}} = k\,\text{Im}[\alpha] = 4\pi k^4 r^3\,\text{Im}\left[\frac{\varepsilon - \varepsilon_m}{\varepsilon + 2\varepsilon_m}\right], \tag{9}$$

$$C_{\text{sca}} = \frac{k^4}{6\pi}|\alpha|^2 = \frac{8\pi}{3}k^4 r^6\left|\frac{\varepsilon - \varepsilon_m}{\varepsilon + 2\varepsilon_m}\right|^2, \tag{10}$$

where k is the wave vector. Here, the normal incident wavelength is set to 380 nm. As we can see from Fig. 7, with the increase of Al nanoparticle radius, the scattering efficiency of the cross section changes greatly. When the radius of Al particles in the ITO layer is less than 30 nm, the absorption efficiency of the cross section is less than the scattering efficiency. When the radius reaches 30 nm, the scattering and absorption efficiencies are nearly the same. When the radius is larger than 30 nm, the scattering efficiency, which is increasing exponentially, is greater than the absorption efficiency. The critical radius of nanoparticles in the a-Si:H layer is 70 nm. Considering the radius used in this paper, the scattering efficiency in a-Si:H is always less than that in the ITO layer. It is confirmed that the absorption characteristics of structure A are superior to structure B and C in Fig. 5(a).

3.3.2 *Short-circuit current*

The short-circuit current is an important parameter in characterizing solar cells. The short-circuit current of solar cells with different locations of metal NPs can be calculated by[31]

$$J_{\text{sc}} = \int_0^\infty \frac{\text{d}j_{\text{sc}}}{\text{d}\lambda}\text{d}\lambda = \int_0^\infty j_{\text{sc}}(\lambda)\text{d}\lambda, \tag{11}$$

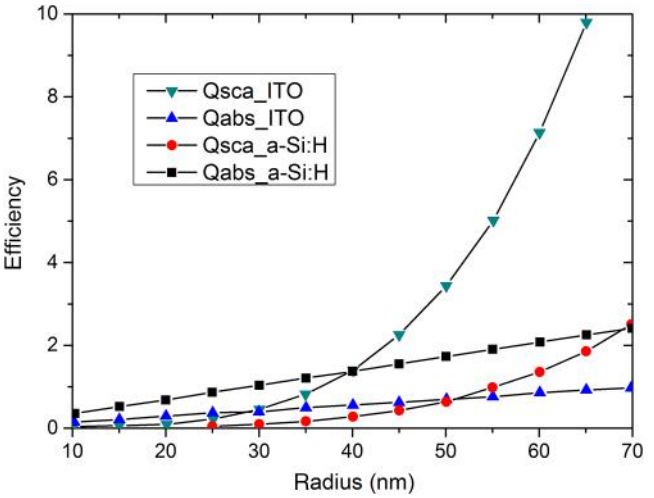

Fig. 7 The relation of scattering efficiency C_{sca} and absorption efficiency C_{abs} with radiuses of Al NPs in the ITO or a-Si:H layer.

$$j_{sc}(\lambda) = \frac{q\lambda}{hc}\text{abs}(\lambda)I(\lambda), \tag{12}$$

where h is the Planck constant, q is the electron charge, and c is the speed of light. Equations (11) and (12) assume that the internal quantum efficiency is 1, ignoring the recombination effect of carriers.

It is found that there is basic coincidence between the curves of "A" and "D" from 300 to 550 nm in Fig. 8. In the structure D, there is one more array of nanoparticles embedded in the bottom of the a-Si: H layer, which can enhance the absorption by scattering light and then increase the short-circuit current. The curves "no NP," "B," and "C" are substantially coincident from 300 to 500 nm, and a larger difference occurs in the wavelength greater than 500 nm.

Table 4 shows that the short-circuit current enhancement of Al NPs deposited on the bottom of the a-Si:H layer, which is shown in Fig. 5(a) as structure C, is one order of magnitude smaller than that of Al nanoparticles deposited in other locations. Because the Al NPs deposited at the bottom of the active layer mainly act on photons of longer wavelengths,

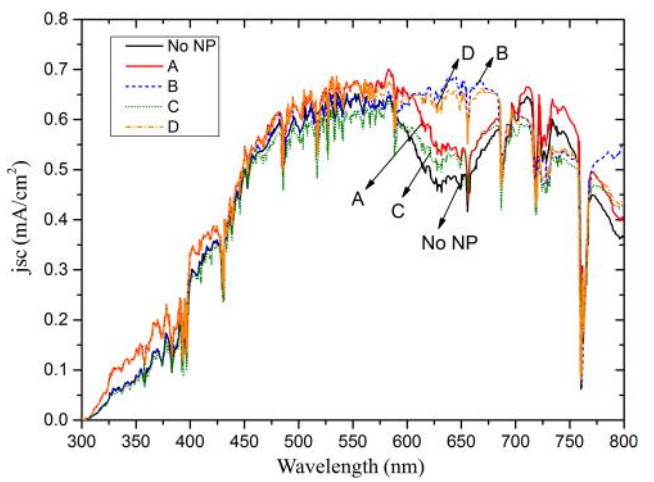

Fig. 8 Short-circuit current of solar cells in the four different structures above.

Table 4 Short-circuit current and the enhanced ratio of short-circuit current of solar cells with nanoparticles at different positions.

Nanoparticle position	Short-circuit current J_{sc} (mA/cm^2)	Enhanced ratio of short-circuit current (%)
no NP	21.32	—
A	23.52	10.32
B	23.18	8.72
C	21.42	0.047
D	23.73	11.31

the spectral energy of this part of the photon is small and contributes less to the short-circuit current. The short-circuit current enhancement of structure A and D is relatively large due to the forming of a graded refractive index structure in the ITO layer, which can enhance the antireflection effect and make the short-circuit current enhancement more obviously. Based on the data in Table 4, it is confirmed that the absorption characteristics of structure D are superior to the others.

4 Conclusions

In this paper, we have studied ways to increase the energy that transfers into the active layer and reduce the parasitic absorption of the nanoparticles themselves in the largest intensity region of the irradiation spectrum. The material property, size, and locations of nanoparticles have been arranged according to the spectral absorption characteristics calculated using the FDTD method.

By analyzing different metals, it is found that Al nanoparticles have the greatest effect on the absorption. Meanwhile, the absorption of Al nanoparticles themselves is relatively weak, which scatters more incident light on the surface. Average absorption is enhanced owing to the increased photon absorption. The absorption enhancement of 300 to 800 nm wavelength light is strongest when the Al particle radius is 30 nm. A structure with deposited metal nanoparticles on the bottom of the a-Si:H layer and the bottom of the ITO layer was found to have superior optical absorption to the other structures investigated. Therefore, we can optimize the structure of thin-film solar cells through tuning the parameters of metal nanoparticles to improve their efficiency.

Acknowledgments

This work was supported by the Fundamental Research Funds for the Central Universities (Grant No. NS2012038), the National Natural Science Foundation of China (Grant No. 51506085), the Natural Science Foundation of Jiangsu Province (Grant No. BK20150742), and the Postdoctoral Foundation of Jiangsu Province (Grant No. 1402048B)

References

1. T. Markvart and L. Castañer, *Practical Handbook of Photovoltaics: Fundamentals and Applications*, Elsevier, Amsterdam (2003).
2. X. Chen et al., "Broadband enhancement in thin-film amorphous silicon solar cells enabled by nucleated silver nanoparticles," *Nano Lett.* **12**(5), 2187–2192 (2012).
3. K. X. Wang et al., "Absorption enhancement in ultrathin solar cells with antireflection and light-trapping nanocone gratings," *Nano Lett.* **12**(3), 1616–1619 (2012).

4. J. Eisenlohr et al., "Rear side sphere gratings for improved light trapping in crystalline silicon single junction and silicon-based tandem solar cells," *Sol. Energy Mater. Sol. Cells* **142**, 60–65 (2015).
5. O. Isabella et al., "3-D optical modeling of thin-film silicon solar cells on diffraction gratings," *Prog. Photovolt. Res. Appl.* **21**(1), 94–108 (2013).
6. M. G. Deceglie et al., "Design of nanostructured solar cells using coupled optical and electrical modeling," *Nano Lett.* **12**(6), 2894–2900 (2012).
7. L. Yang, Y. Xuan, and J. Tan, "Efficient optical absorption in thin-film solar cells," *Opt. Express* **19**(5), A1165 (2011).
8. W. Wang, "Broadband light absorption enhancement in thin-film silicon solar cells," *Nano Lett.* **10**(6), 2012–2018 (2010).
9. M. L. Brongersma, Y. Cui, and S. Fan, "Light management for photovoltaics using high-index nanostructures," *Nat. Mater.* **13**, 451–460 (2014).
10. F. Hallermann et al., "On the use of localized plasmon polaritons in solar cells," *Phys. Status Solidi A* **205**(12), 2844–2861 (2008).
11. H. A. Atwate and A. Polman, "Plasmonics for improved photovoltaic devices," *Nat. Mater.* **9**(3), 205–213 (2010).
12. K. R. Catchpole and A. Polman, "Plasmonic solar cells," *Opt. Express* **16**(26), 21793 (2008).
13. I. M. Pryce et al., "Plasmonic nanoparticle enhanced photocurrent in GaN/InGaN/GaN quantum well solar cells," *Appl. Phys. Lett.* **96**(15), 153501 (2010).
14. K. R. Catchpolea and A. Polman, "Design principles for particle plasmon enhanced solar cells," *Appl. Phys. Lett.* **93**(19), 191113 (2008).
15. Y. Zhang et al., "Towards ultra-thin plasmonic silicon wafer solar cells with minimized efficiency loss," *Sci. Rep.* **4**, 4939 (2014).
16. Y. Zhang et al., "Low cost and high performance Al nanoparticles for broadband light trapping in Si wafer solar cells," *Appl. Phys. Lett.* **100**(15), 151101 (2012).
17. Y. A. Akimov and W. S. Koh, "Resonant and nonresonant plasmonic nanoparticle enhancement for thin-film silicon solar cells," *Nanotechnology* **21**(23), 235201 (2010)
18. N. F. Fahim et al., "Enhanced photocurrent in crystalline silicon solar cells by hybrid plasmonic antireflection coatings," *Appl. Phys. Lett.* **101**(26), 261102 (2012).
19. N. Fahim et al., "Efficiency enhancement of screen-printed multicrystalline silicon solar cells by integrating gold nanoparticles via a dip coating process," *Opt. Mat. Express* **2**(2), 190–204 (2012).
20. F. Parveen et al., "Copper nanoparticles: Synthesis methods and its light harvesting performance," *Sol. Energy Mater. Sol. Cells* **144**, 371–382 (2016).
21. B. Cai et al., "Near-field light concentration of ultra-small metallic nanoparticles for absorption enhancement in a-Si solar cells." *Appl. Phys. Lett.* **102**(9), 093107 (2013).
22. S. Wu et al., "Absorption enhancement in thin-film silicon solar cells by two-dimensional periodic nanopatterns," *J. Nanophoton.* **4**(1), 043515 (2010).
23. D. Zhang et al., "Aluminum nanoparticles enhanced light absorption in silicon solar cell by surface plasmon resonance," *Opt. Quant. Electron.* **47**(6), 1421–1427 (2015)
24. D. Fleisch, *A Student's Guide to Maxwell's Equations*, Cambridge University Press, Cambridge (2008).
25. D. B. Ge and Y. B. Yan, *The Finite Difference Time Domain Method for Electromagnetic Wave*, Xi' an Electronic and Science University Press, Xi' an (2005).
26. E. D. Palik, *Handbook of Optical Constants of Solids*, Vol. **3**, Academic Press, Salt Lake City (1998).
27. Y. A. Akimov, W. S. Koh, and K. Ostrikov, "Enhancement of optical absorption in thin-film solar cells through the excitation of higher-order nanoparticle plasmon modes," *Opt. Express* **17**(12), 10195 (2009).
28. G. Mie, "Beitrage Zur Optik Truber Medien, Speziell Kolloidaler Metallosungen," *Ann. Phys.* **330**(3), 377–445 (1908).
29. S. A. Maier, *Plasmonics: Fundamentals and Applications*, Springer Science, New York (2007).
30. C. F. Bohren and D. R. Huffman, *Absorption and Scattering of Light by Small Particles*, Wiley, New York (1983).
31. S. Zanotto et al., "Light trapping regimes in thin-film silicon solar cells with a photonic pattern," *Opt. Express* **18**(5), 4260–4274 (2010).

Bo Shi received his PhD in mechanical engineering from the University of California, Los Angeles, in 2006. He is currently an associate professor at Nanjing University of Aeronautics and Astronautics. His current scientific interests are focused on the heat transfer and energy conversion of micro/nanoscale.

Wei Wang is currently a master degree candidate at Nanjing University of Aeronautics and Astronautics. Her current scientific interests are focused on the utilization and conversion of solar energy.

Xueqing Yu is a master degree candidate at Nanjing University of Aeronautics and Astronautics. Her scientific interests are focused on the surface nanostructure of solar cells.

Lili Yang received her PhD in engineering thermophysics from Nanjing University of Science and Technology in 2013. She is currently a lecturer at Nanjing University of Aeronautics and Astronautics. Her current scientific interests are focused on the technology of efficient photovoltaic solar cells.

Yuanpei Xu is currently a doctoral candidate at Nanjing University of Aeronautics and Astronautics. His current scientific interests are focused on the photon management for solar cells.